This document is confidential and is proprietary to the American Chemical Society and its authors. Do not copy or disclose without written permission. If you have received this item in error, notify the sender and delete all copies.

CrN, CuB, and AuB: A Tale of Two Dissociation Limits

Journal:	The Journal of Physical Chemistry Letters
Manuscript ID	jz-2023-01712a.R1
Manuscript Type:	Letter
Date Submitted by the Author:	31-Jul-2023
Complete List of Authors:	Merriles, Dakota; University of Utah, Department of Chemistry Morse, Michael; University of Utah, Department of Chemistry



CrN, CuB, and AuB: A Tale of Two Dissociation

Limits

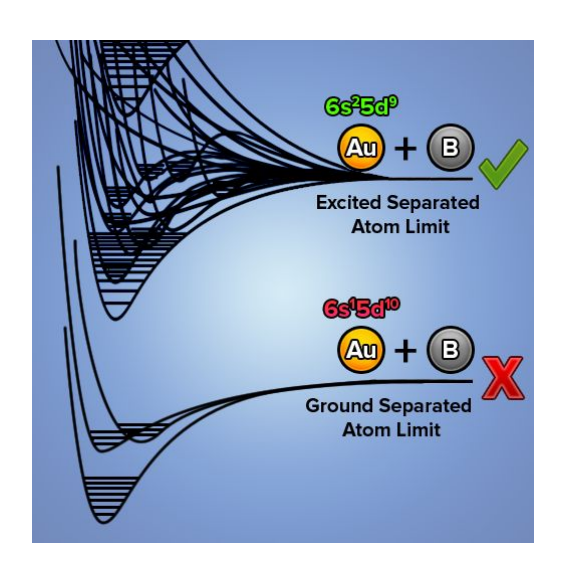
Dakota M. Merriles and Michael D. Morse*

Department of Chemistry, University of Utah, Salt Lake City, Utah 84112

*Corresponding Author Email: morse@chem.utah.edu

ABSTRACT: Predissociation thresholds corresponding to dissociation at ground state separated atom limits (SALs) have been recorded in this group for over 100 d- and f-block metal-containing molecules. The metal atom electronic degeneracies in these molecules generate a dense manifold of electronic states that allow high-lying vibronic levels to couple to pathways leading to dissociation. However, CrN, CuB, and AuB fail to dissociate at their ground SAL. Instead, the molecules remain bound at energies that far surpass their bond dissociation energies (BDEs) and their bonds break only when excited at or above an excited SAL. Sharp predissociation thresholds at excited SALs nevertheless allowed BDEs to be derived: $D_0(CrN)$: 3.941(22) eV, $D_0(CuB)$: 2.26(15) eV, and $D_0(Au^{11}B)$: 3.724(3) eV. A previous measurement of $D_0(AlCr)$ is re-evaluated as dissociating to a higher energy limit, giving a revised value of $D_0(AlCr) = 1.32(2)$ eV. A discussion of this physical behavior is presented.

TOC GRAPHIC



KEYWORDS: Predissociation, Metals, Transition Metals, Molecules, Quantum Mechanics, Bond Dissociation Energies

The phenomenon of predissociation was first proposed nearly 100 years ago by Henri and Teves based on the absorption spectrum of S₂: "...the molecule can be modified in its internal structure: the atoms are driven apart, the bonds are weakened, the molecule becomes more reactive, and the rotational movements are no longer quantified. This first modification is a preliminary preparation of the molecule for its total dissociation, and it is necessary to introduce a new term for this change. We propose to denote it by the term *predissociation* of the molecule." Since then, quantitative descriptions of predissociation have been the objective of experimental and theoretical studies. ²⁻⁷ The defining characteristic of predissociation is that a molecule excited to a particular electronic state dissociates at energies below the corresponding separated atom limit (SAL) for that state. In other words, imagine a molecule that is excited to a vibronic level in an electronic state that emanates from an excited separated atom limit. If this vibronic level can be coupled to a lower energy SAL through a perturbation, the molecule can fall apart in a collisionless, nonradiative manner well below the energy of the SAL from which the initially excited vibronic level derives. This process is molecular predissociation.

When a small number of electronic states exists near the ground SAL, a molecule excited to these states is unlikely to predissociate at the thermochemical threshold because of poor coupling among the limited number of states. Instead of finding a pathway to dissociation, the molecule will remain bound and eventually radiatively decay into a lower-lying vibronic level. On the contrary, when a dense manifold of vibronic states is present at a SAL, as must occur for SALs arising from atoms with highly degenerate states, *i.e.* most open *d*- or *f*-shell metal atoms, dissociative pathways from these vibronic levels *via* predissociation can occur as soon as the process becomes energetically possible.

Our group has taken advantage of the predissociation phenomenon to measure highly precise bond dissociation energies (BDEs) of a wide variety of small, open subshell d- and fblock molecules using resonant two-photon ionization (R2PI) spectroscopy.⁸ In these experiments, the molecule of interest is probed in a low-pressure (10⁻⁶ Torr), collision-free environment where a laser pulse excites it into a quasi-continuum of vibronic states just below the ground SAL. Absorption of a second photon, from the same or a different laser pulse, then ionizes the molecule and ions are detected in a mass spectrometer. As we increase the excitation energy, the predissociation threshold is eventually observed when the molecule has sufficient excitation energy to find a pathway to dissociation via spin-orbit and nonadiabatic couplings. The predissociation threshold of the molecule, i.e., the cue that the chemical bond in the molecule has been broken, is noted as a sharp drop in ion signal to a zero baseline as the excitation laser is scanned to higher energies. The sharp drop in ion signal occurs because predissociation often occurs on a subnanosecond time scale, so the molecule falls apart faster than it can be ionized. When the predissociation process isn't quite so rapid, the predissociation threshold can still be reliably observed if the ionization photon is delayed. In the present experiments, a 40 ns delay is employed to give the excited molecules sufficient time to dissociate. Thermochemical cycles grounded in the first law of thermodynamics relate pertinent properties of molecules, like BDEs of neutral, ionized, and anionic molecules. When predissociation-based BDE values are employed in these thermochemical cycles, excellent selfconsistency is obtained, confirming the validity of this method of measuring BDEs.

Following our initial observation that sharp predissociation thresholds can be used to measure accurate and precise BDEs of small *d*- and *f*-block molecules, ¹⁰ we have worked toward building a comprehensive database of BDEs for these molecules. In the process, the

requirements that must be met to use predissociation thresholds to measure BDEs accurately have been extensively discussed. 11-14 The most important requirement is that a high density of electronic states must exist in the vicinity of the ground SAL. Usually, the electronic degeneracies imparted by the open *d*- and *f*-subshells in the metal atomic fragment guarantees that the molecule will have a sufficient density of electronic states for predissociation to occur at threshold.

Recently, we were able to measure the sharp predissociation threshold of YbO in an R2PI experiment, and were able to assign the threshold as the BDE of the molecule. 11 Originally, we thought this could not be achieved because the ground SAL for YbO, Yb (${}^{1}S_{g}$, $6s^{2}$ 4f 14) + O (${}^{3}P_{g}$, $2s^{2}$ 2p 4), 15 only generates nine electronic states due to the closed shell character of the Yb atom. 16 The small number of electronic states arising from this limit could lead one to expect a fairly discrete electronic spectrum near the ground SAL with predissociation dynamics similar to that found in the well-studied predissociations of p-block diatomic molecules. 7 Instead, a high density of electronic states was observed with a sharp and unambiguous predissociation threshold. Ultimately, this unexpected behavior in YbO was reconciled by the recognition that strongly bound electronic states originating from Yb $^{+}$ + O $^{-}$ and Yb $^{2+}$ + O $^{2-}$ separated ion limits drop into the energetic vicinity of the ground SAL, furnishing a sufficient density of states for spin-orbit and nonadiabatic coupling mechanisms to provide a pathway to rapid dissociation.

In the current work, we present three examples of transition metal-*p*-block diatomics that fail to predissociate at their ground SAL, instead remaining intact until an excited SAL becomes energetically accessible. Diatomic CrN, CuB, and AuB all demonstrated this physical behavior during spectroscopic studies directed toward predissociation-based measurements of their BDEs. Intense molecular ion signals and high densities of vibronic states were observed at excitation

energies that greatly surpassed the expected BDEs of these species. While the metal atomic constituents of these molecules are all different, their ground atomic terms all lack orbital angular momentum (L=0). This is the key fact that reduces the density of states at the ground SAL sufficiently to prevent predissociation at the thermochemical threshold. Further exacerbating this situation for CrN is that the nitrogen atomic ground state also lacks orbital angular momentum (L=0), so that the ground SAL for CrN exhibits no M_L degeneracy and has only spin degeneracy.

Figure 1 displays the R2PI spectrum and predissociation threshold of CrN. The breakoff in CrN⁺ ion signal occurs at 39,455(100) cm⁻¹ (4.892(12) eV). A red line has been drawn at the right side of the molecular ion signal curve corresponding to zero signal in Figs. 1-3. Assigning the observed predissociation threshold as the CrN BDE would make it one of the most strongly bound of the 3d MN molecules, ¹⁷ nearly equaling the BDEs of TiN (5.000(19) eV) and VN (4.997(2) eV). ^{17, 18} For CrN to have a BDE comparable to TiN and VN would be unexpected because the half-filled 3d shell of Cr is greatly stabilized by exchange effects that are destroyed when the 3d electrons are spin-paired with the 2p electrons of N to form bonds. The large exchange stabilization of the Cr ground state causes CrX molecules to uniformly exhibit weaker bonds than the corresponding VX molecules, as measured or computed for the VX and CrX molecules, where X = B, C, O, F, Si, P, S, and Cl. Moreover, a calculation of the CrN BDE using CCSD(T) theory extrapolated to the complete basis set limit (CBS) (See Supporting Information, Table S1) obtains a BDE of 3.62 eV for CrN, 1.27 eV lower than the predissociation threshold found in Figure 1. The MOs of CrN, CuB, and AuB are described in the SI and a MO diagram for AuB is presented in Figure S1.

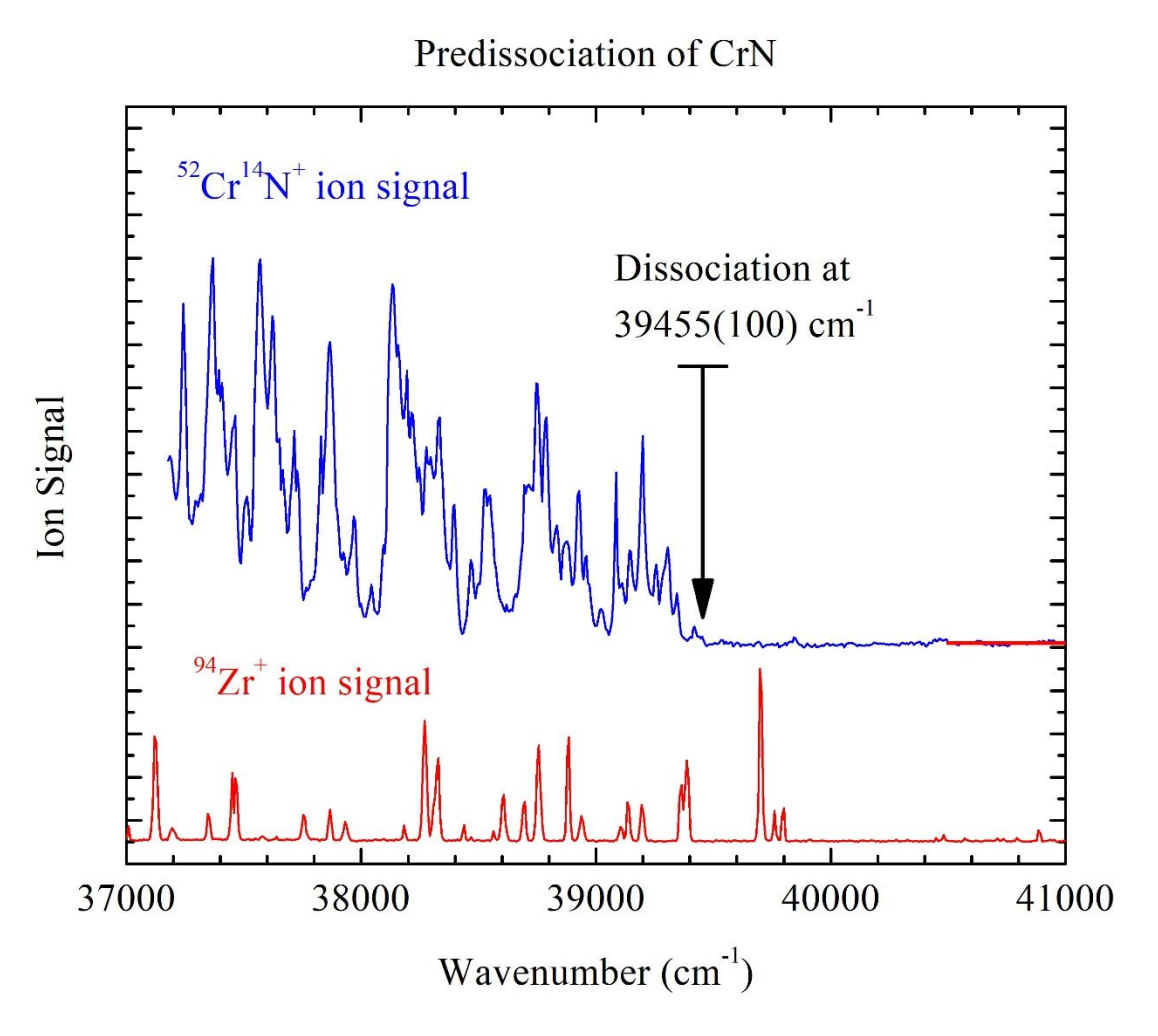


Figure 1. R2PI spectrum of CrN and its dissociation to an excited SAL. The upper, blue trace displays the measured ⁵²Cr¹⁴N ion signal and its predissociation threshold at 39 455(100) cm⁻¹. The lower, red trace displays the ⁹⁴Zr atomic signal that was used to calibrate the spectrum.

If the predissociation threshold in Figure 1 is instead interpreted as CrN finding a pathway to dissociation at an excited SAL, assigning a BDE to CrN from this spectrum becomes possible. The first and second excited SALs of CrN are located 7593.15 cm⁻¹ and 7750.75 cm⁻¹ above the ground SAL and correspond to Cr in its ${}^5S_{2g}$, $3d^54s^1$ and ${}^5D_{0g}$, $3d^44s^2$ electronic configurations, respectively. Additional Cr* ${}^5D_{Jg}$ levels (J = 1, 2, 3, 4) lie at energies of 7810.78 to 8307.58 cm⁻¹. Potential curves descending from these SALs add to the density of

electronic states at the Cr* $^5D_{0g}$ + N $^4S_{3/2u}$ limit, increasing the likelihood of predissociation to that limit. From the ground $^4\Sigma^-_{1/2,\,3/2}$ state of CrN, transitions to states with $\Omega=1/2,\,3/2$, and 5/2 are allowed. Perturbations due to spin-orbit interaction, nonadiabatic effects, and the L- and S-uncoupling operators allow these excited levels to predissociate at either the Cr* $^5S_{2g}$ + N $^4S_{3/2u}$ or the Cr* $^5D_{0g}$ + N $^4S_{3/2u}$ SALs, so it is unlikely that predissociation would fail to occur until the higher energy spin-orbit levels of the Cr* 5D_g term are reached. The next SAL above these limits lies about 1.4 eV higher in energy and cannot correspond to the observed predissociation threshold, as it would lead to a BDE that is far too low. Determining the SAL to which the CrN molecules dissociate in Figure 1 is difficult because of the small (158 cm⁻¹) difference in their energies.

The high density of electronic states at the observed predissociation threshold evident in Figure 1 suggests that pathways would be available for the molecule to dissociate at the lower of these two SALs. Accordingly, we suspect that the BDE of CrN is given by the difference of the measured predissociation threshold, 39,455(100) cm⁻¹ and the energy of the Cr* ${}^5S_{2g}$, $3d^54s^1 + N$ 2p³, ${}^4S_{3/2u}$ separated atom limit, 7593.15 cm⁻¹. This would place the BDE of CrN at 31,862(100) cm⁻¹ or 3.950(12) eV. However, this limit only generates ${}^{2,4,6,8}\Sigma^-$ molecular states, limiting the pathways available to dissociation. 16 As a result, it is possible that predissociation fails to occur in CrN until the energy of the higher lying Cr* ${}^5D_{0g}$, $3d^44s^2 + N$ 2p³, ${}^4S_{3/2u}$ limit is reached at 7750.75 cm⁻¹. Despite this concern, the even smaller number of states correlating to the ground SAL in YbO (only ${}^3\Sigma^-$ and ${}^3\Pi$) did not prevent rapid predissociation to this limit, allowing the BDE of YbO to be precisely measured. 11 Like YbO, the high density of states found in the spectrum of CrN displayed in Figure 1 is likely due to ion pair states, in this case diabatically correlating to Cr* 4 3d 5 , 6 Sg + N ${}^-$, 2p4, 3 Pg, which drop down into the energetic region spanned in

Figure 1. Indeed, previous spectroscopic work has identified the $A^4\Pi$ and $B^4\Sigma^-$ states near 13,500 cm⁻¹ and 20,500 cm⁻¹, respectively.^{28,29} These states leave the 4s-like 9σ orbital of CrN vacant, and probably correlate diabatically to the Cr⁺ 3d⁵, $^6S_g + N^-$, $2p^4$, 3P_g ion pair limit. Additional ion-pair states deriving from the Cr⁺ 3d⁴4s¹, ⁶D_g + N⁻, 2p⁴, ³P_g ion pair limit, approximately 12,000 cm⁻¹ higher in energy also undoubtedly drop into the region spanned by Figure 1.

Although these considerations cause us to suspect that predissociation occurs at the Cr* ${}^5S_{2g}$, $3d^54s^1 + N 2p^3$, ${}^4S_{3/2u}$ atomic limit, the possibility remains that rapid predissociation doesn't set in until the Cr* $^5D_{0g}$, $3d^44s^2 + N ^4S_{3/2u}$, $2p^3$ limit is reached at 7750.75 cm⁻¹. This would place the CrN BDE at 39,455(100) - 7750.75 cm⁻¹ = 31,704(100) cm⁻¹, or 3.931(12) eV. To be conservative, we assign the CrN BDE as the average of these two values with suitably expanded error limits, as $D_0(CrN) = 3.941(22) \text{ eV}$.

Figure 2 displays the predissociation threshold in CuB at 30 490(150) cm⁻¹ or 3.780(19) eV. Like CrN, an assignment of the CuB BDE to this threshold would give CuB an abnormally large bond energy. BDEs for Cu based diatomic molecules that are bonded to 2p-block elements are uniformly smaller than their analogous Ni-2p diatomics.³⁰⁻³³ Notably, the difference of the BDEs becomes even larger as the electronegativity of the 2p block element decreases. The BDE of NiB has been measured to be 3.431(4) eV,34 so an assignment of 3.780(19) eV to the CuB BDE would violate the established $D_0(NiX) >> D_0(CuX)$ trend for 2p ligands. Moreover, highlevel MRCI+O calculations predict $D_0(CuB) = 2.10 \text{ eV}$ or 2.18 eV. 35, 36 In the current work, CCSD(T)/CBS calculations give $D_0(CuB) = 2.26$ eV (See Supporting Information, Table S1). All of these are far less than the 3.780(19) eV predissociation threshold of Figure 2. Looking at the separated atom limits of this system, however, four possible SALs can combine with the measured predissociation threshold to give BDEs between 0.25 eV (ridiculously too low) and

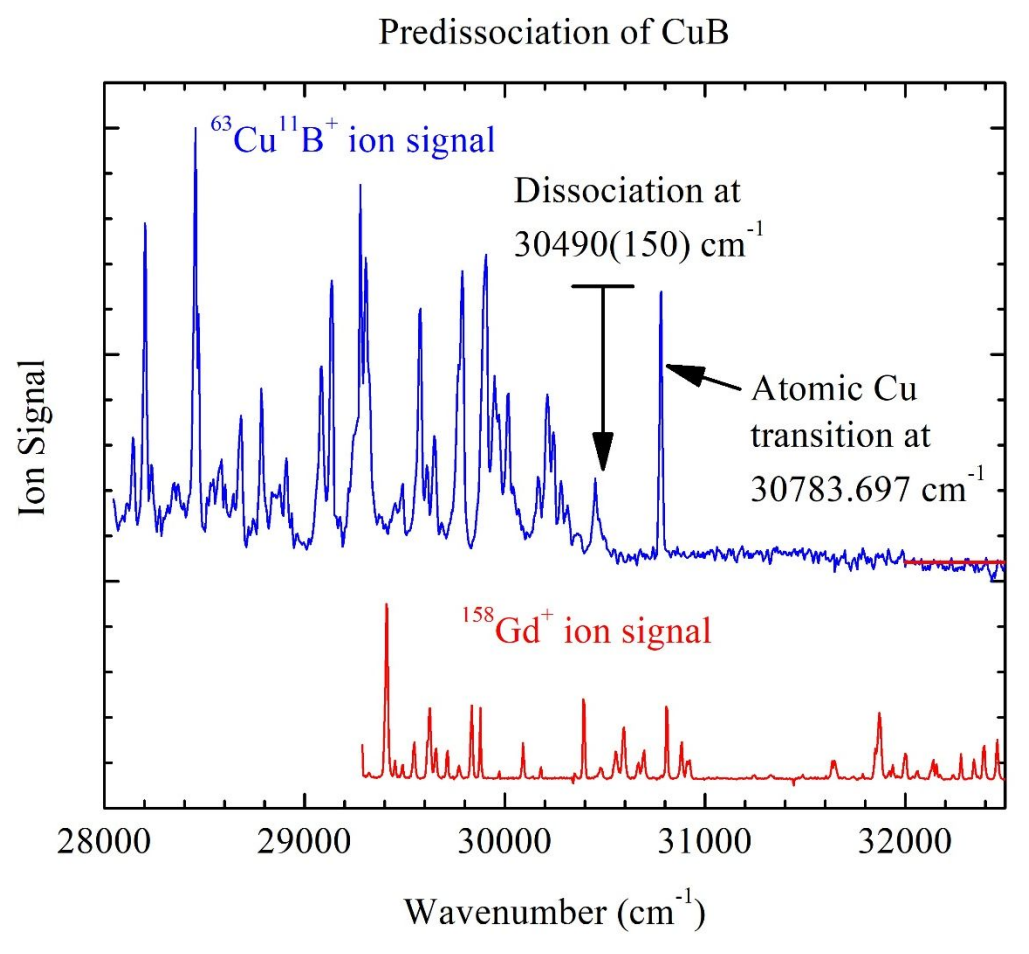


Figure 2. R2PI spectrum of CuB in the vicinity of its predissociation to an excited SAL. The top, blue trace displays the ⁶³Cu¹¹B signal and its measured predissociation threshold at 30,490(150) cm⁻¹ or 3.780(19) eV. Also observed is a strongly allowed Cu atomic transition at 30 783.697 cm⁻¹ that caused an artificial increase in signal for CuB.¹⁵ This is an unavoidable artifact of the R2PI technique.³⁷ The bottom, red trace shows the ¹⁵⁸Gd atomic transitions that were used to calibrate the wavenumber axis.

3.75 eV (far too high). These are the Cu* (${}^{2}D_{Jg}$, 4s² 3d⁹, J = 5/2, 3/2) + B (${}^{2}P_{J'u}$, 2s² 2p¹, J'=1/2, 3/2) limits, which lie at energies 1.389 to 1.644 eV above the ground limit. Subtracting these SAL energies from the measured predissociation threshold places the BDE of CuB in the range of 2.136 to 2.391 eV. As in the case of CrN, we suspect that the CuB molecule predissociates at the lowest of these limits, giving $D_{0}(CuB) = 2.391(19)$ eV. The more conservative option,

however, averages the outer limits of this range and increases the error limit appropriately to provide $D_0(CuB) = 2.26(15)$ eV, which agrees with all high-quality computations to within the error limit. To the best of our knowledge, this marks the first experimental study of CuB as well as the first time a predissociation threshold has been used to measure the BDE of a neutral copper-containing molecule.

Figure 3 displays the R2PI spectra for both isotopologues of AuB in the vicinity of their predissociation thresholds. During the R2PI experiment for AuB, both ¹⁹⁷Au¹¹B and ¹⁹⁷Au¹⁰B signals were recorded with excellent signal-to-noise ratios, allowing predissociation thresholds to be measured for both species. The threshold for ¹⁹⁷Au¹⁰B was found to be 20 cm⁻¹ lower than that of ¹⁹⁷Au¹¹B, in accord with the higher zero-point energy of the lighter species. Employing the harmonic approximation and a previously reported vibrational frequency of 704 cm⁻¹ for ¹⁹⁷Au¹⁰B, ³⁸ the calculated vibrational frequency of ¹⁹⁷Au¹¹B is found to be 674 cm⁻¹, leading to an expected zero-point energy difference of roughly 15 cm⁻¹. Within expected precision, this is in good agreement with the 20 cm⁻¹ difference between the measured predissociation thresholds.

The predissociation thresholds for ¹⁹⁷Au¹¹B and ¹⁹⁷Au¹⁰B are 4.861(2) eV and 4.859(2) eV, respectively. If these corresponded to AuB undergoing predissociation at its ground SAL, AuB would be nearly as strongly bound as the most strongly bound transition metal borides, RuB, RhB, IrB, and PtB.³⁴ This would be unexpected because the 5d orbitals of Au are energetically buried, leading to weakened bonds with p-block elements. Significantly weakened bonding in AuX molecules compared to RuX, RhX, IrX, and PtX molecules has been demonstrated in numerous measurements and calculations.^{30, 39-42} Alternatively, if the threshold in Figure 3 is assigned as AuB predissociating to its first excited SAL of Au* (²D_{5/2g}, 6s² 5d⁹) + B (²P_{1/2u}, 2s² 2p¹) located 1.136 eV higher in energy than its ground SAL, ¹⁵ BDEs of

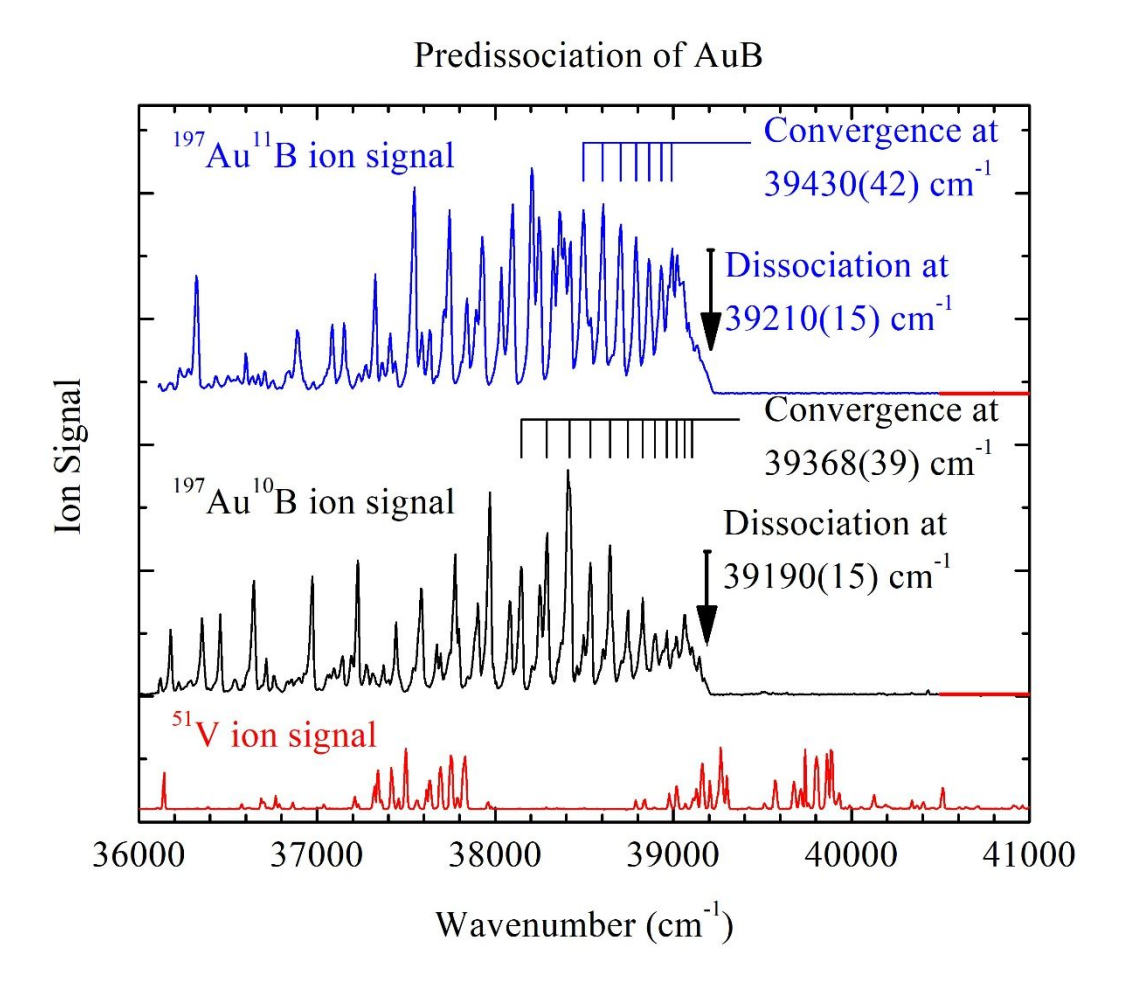


Figure 3. R2PI Spectrum of AuB in the energetic vicinity of its dissociation to the first excited limit of Au 5d⁹6s², ²D_{5/2g} + B 2p¹, ²P_{1/2, 3/2u}. The top, blue trace displays the ¹⁹⁷Au¹¹B⁺ ion signal and its predissociation threshold at 39 210(15) cm⁻¹ or 4.861(2) eV. The middle, black trace shows the ¹⁹⁷Au¹⁰B⁺ ion signal and its predissociation threshold at 39 190(15) cm⁻¹ or 4.859(2) eV. Vibrational progressions are identified above each spectrum and their convergence limits are listed. The bottom, red trace shows the ⁵¹V atomic spectrum that was collected for calibration.

 $D_0(^{197}Au^{11}B) = 3.725(2)$ eV and $D_0(^{197}Au^{10}B) = 3.723(2)$ eV are obtained. The SAL corresponding to spin-orbit excited boron lies only 15.287 cm⁻¹ higher, reducing these values by 0.002 eV if dissociation occurs to this limit. The next higher separated atom limit lies 1.52 eV higher, which would reduce the AuB BDE to an unacceptably low value. Averaging the BDEs

obtained for dissociation to the two different boron spin states and increasing the error limit appropriately, we obtain final values of the BDE of 197 Au 11 B and 197 Au 10 B of 3.724(3) eV and 3.722(3) eV, respectively. These are in excellent agreement with a Knudsen effusion measurement of $D_0(AuB) = 3.77(11)$ eV. 43 Moreover, a calculation using the CCSD(T)/CBS methodology in the current study gives a BDE of 3.75 eV for AuB, in excellent agreement with these results (See Supplementary Information, Table S1). Therefore, we assign the thresholds in Figure 3 to be representative of AuB predissociating at its first excited SAL and report the BDEs as $D_0(Au^{10}B) = 3.722(3)$ eV and $D_0(Au^{11}B) = 3.724(3)$ eV.

In the R2PI spectra of the AuB isotopologues, a vibrational progression was identified, with its members indicated in Figure 3. These vibronic transitions were fitted to a Birge-Sponer extrapolation⁴⁴ with a simple linear fit to estimate the dissociation energy of the isotopologues: 39430(42) cm⁻¹ and 39368(39) cm⁻¹ for ¹⁹⁷Au¹¹B and ¹⁹⁷Au¹⁰B, respectively. These extrapolations are displayed in Figure 4. The difference between the two values is 62 cm⁻¹, much larger than the 20 cm⁻¹ difference between their predissociation limits and also much larger than the expected 15 cm⁻¹ difference between the zero-point energies. However, a combined error of 57 cm⁻¹ for the two extrapolations is obtained, rendering the large difference between their convergence limits moot.

It is interesting that the extrapolated dissociation limits exceed the observed predissociation thresholds by 220(45) cm⁻¹ and 178(42) cm⁻¹ for ¹⁹⁷Au¹¹B and ¹⁹⁷Au¹⁰B, respectively. One could rationalize this difference by simply noting that Birge-Sponer extrapolations are often unreliable, ^{21, 45, 46} but this would require that the last few unobserved vibrational levels converge to the limit far more quickly than the Morse potential form provides.

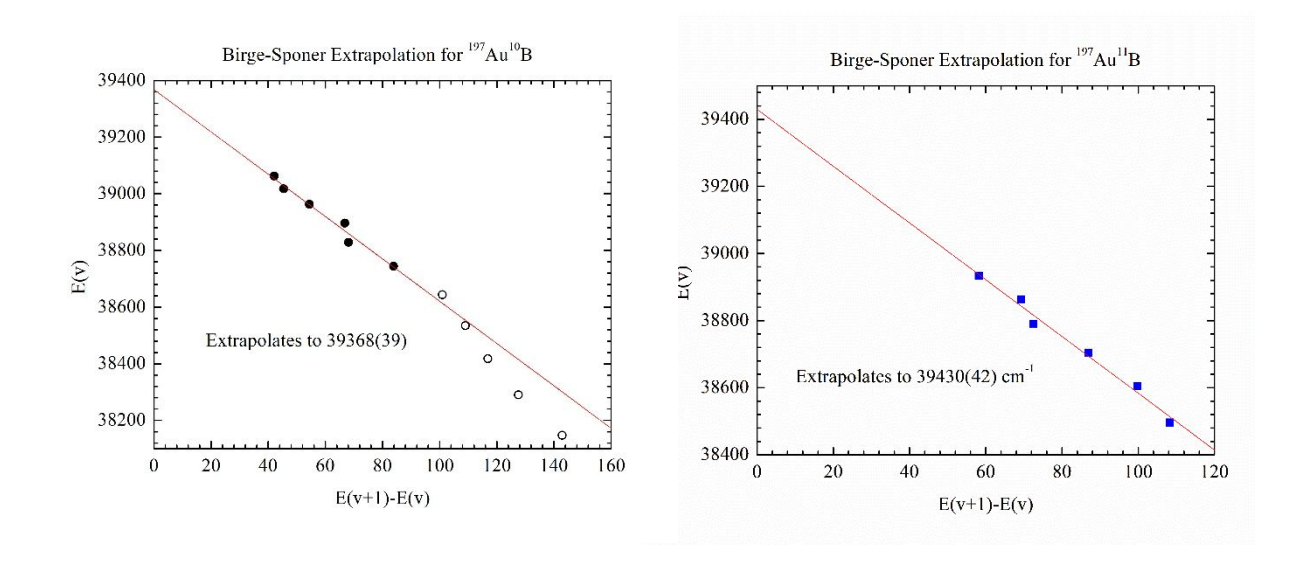


Figure 4. Left: The Birge-Sponer extrapolation performed for ¹⁹⁷Au¹⁰B, converging at 39 368(39) cm⁻¹. A total of 11 vibrational features were identified as part of the vibrational progression, represented by the 11 black circles. The six filled black circles were used in the linear fit, as the five unfilled black circles display a notably different slope. Right: The Birge-Sponer extrapolation performed for ¹⁹⁷Au¹¹B, converging at 39 368(39) cm⁻¹. The six blue squares represent the six vibrational features identified in the ¹⁹⁷Au¹¹B R2PI spectrum.

Another possibility is that the electronic state responsible for the fitted progression may have a barrier to dissociation, causing the fitted vibrational levels to extrapolate to the top of the barrier, rather than to the SAL. Such a barrier could in some cases prevent dissociation at the energy of the SAL, invalidating the assignment of the AuB BDE. The observation of predissociation at an energy below this extrapolated limit, however, shows that dissociation below the top of the barrier can readily occur, presumably by coupling to other electronic states that dissociate to the same limit but lack a barrier. A possible explanation of these observations is that the vibrational progression occurs in an optically allowed $^{1}\Sigma^{+}$ state in which the 2p electron of the boron atom approaches the gold atom in a p σ orientation. A long-range repulsive interaction with the 6s² electrons could cause the potential curve to exhibit a barrier before becoming attractive when the 2p σ electron interacts with an unpaired 5d σ electron in the 5d σ core to form a bond. In contrast, if the B atom approaches in a 2p σ orientation, the initial long-range

interaction should be attractive, as the $6s^2$ electrons of Au may interact in a dative manner with the empty $2p\sigma$ orbital on boron. Spin-orbit or nonadiabatic coupling to a long-range attractive state of this type could then provide a mechanism for a $^1\Sigma^+$ state with a barrier to predissociate at threshold. Detailed calculations of the potential energy curves in this system will be required to validate this mechanism, which is only presented as a conjecture. Regardless, it appears that the observed predissociation thresholds, minus the energy of the separated atom limits, provide a valid measure of the BDE of diatomic AuB.

These results for CrN, CuB, and AuB suggest that our previous measurement of the BDE of AlCr, which was assigned based on a predissociation threshold in a highly congested vibronic spectrum, may be in error.⁴⁷ In the previous investigation, the BDE of AlCr was assigned as $D_0(AlCr) = 2.272(9)$ eV, a value that is similar to the BDEs of late 3d transition metal aluminide molecules, $D_0(AlCo) = 1.844(2)$ eV and $D_0(AlNi) = 2.29(5)$ eV.^{47, 48} Subsequent density functional (B3LYP) calculations on the BDE of AlCr gave bond energies much lower in energy than our measurement: 1.17 eV and 1.11 eV.^{39,49} With the knowledge gained from the current experiments on CrN, CuB, and AuB, we postulate that the observed predissociation threshold of AlCr corresponds to the molecule dissociating to either the Al $3s^23p^1$, ${}^2P_{1/2u,3/2u} + Cr* 3d^54s^1$, $^{5}S_{2u}$ limits at 7593 or 7705 cm⁻¹ or to the Al $3s^{2}3p^{1}$, $^{2}P_{1/2u,3/2u} + Cr^{*} 3d^{4}4s^{2}$, $^{5}D_{0u}$ limits at 7750 or 7862 cm⁻¹, rather than to the ground separated atom limit. Subtracting these SAL energies from the measured predissociation threshold of 18,377(15) cm⁻¹ and adjusting the error limit to encompass all four SALs places the BDE in the range $D_0(AlCr) = 10.649(150)$ cm⁻¹ or $D_0(AlCr)$ = 1.32(2) eV. This value is in reasonable agreement with computations, giving deviations between experimental and computed values that are comparable to those obtained for the other

3d transition metal aluminides AlV, AlCo, AlNi, and AlCu.^{39, 47, 48, 50} It is apparent that our original supposition that predissociation occurred rapidly at the ground SAL was invalid.

In this work, we have shown that molecules with a low density of electronic states at the ground SAL can fail to predissociate at that limit. However, sharp predissociation thresholds at higher energies corresponding to excited SALs can nevertheless be used to deduce the BDEs of these species. The inability of CrN, CuB, AuB, and AlCr to predissociate at their ground SALs runs counter to our observations of every other transition metal-p-block diatomic molecule that we have investigated but is readily explained by the lack of M_L degeneracy in the transition metal atom at this limit, leading to a low density of states arising from this limit. In combination with the large energy gap before the first excited SAL is reached, this prevents predissociation at the ground SAL.

The present work marks the first time diatomic CuB has been experimentally studied and the first BDE measurement for CuB and CrN. Additionally, the newly reported BDE of AuB reduces the error limit from its previous value by a factor of 35. Vibrational progressions in the R2PI spectra of Au¹⁰B/Au¹¹B allowed Birge-Sponer extrapolations to be performed. The convergence limits of these extrapolations surpass the measured predissociation thresholds by about 200 cm⁻¹, suggesting a barrier to dissociation in this particular AuB excited state. However, we argue that other states arising from the same limit will be barrier-free and that coupling to these states allows predissociation to occur when the excited SAL is reached. Moving forward, studying additional metal-p-block molecules where the metals have ground S terms (L=0) is of interest to clarify when predissociation occurs to the ground SAL (as occurs in CrO,²¹ MoN,¹⁷ MoO,²¹ MoS,⁵¹ EuO,¹¹, EuS, ⁵² EuSe,⁵² and YbO¹¹) and when predissociation

fails to occur at the ground SAL but can be observed at an excited SAL (as happens in CrN, CuB, AuB, and AlCr).

ASSOCIATED CONTENT

Supporting Information. The Supporting Information is available free of charge:

<u>CrN_CuB_AuB_SI.pdf</u> – Experimental Methods, Computational Methods, Error Limit

Discussion, MO Diagram for AuB, Measured and Calculated Properties of CrN, CuB, and AuB

<u>CrN_SI.csv</u>, <u>CuB_SI.csv</u>, <u>AuB_SI.csv</u>, and <u>AuB_Birge-Sponer_extrapolation_SI.csv</u> – CSV files containing spectra and data from Figures 1-4.

Notes

The authors declare no competing financial interests.

ACKNOWLEDGMENTS

The authors would like to thank the National Science Foundation for support of this research under Grant No. CHE-1952924. The authors also would like to recognize the Center for High Performance Computing at the University of Utah for their technical resources and support.

REFERENCES

- (1) Henri, V.; Teves, M. C. Absorption Spectrum and Constitution of Sulphur Vapour. Predissociation of Molecules. *Nature* **1924**, *114* (2877), 894-895.
- (2) Rice, O. K. Perturbations in Molecules and The Theory of Predissociation and Diffuse Spectra. *Physical Review* **1929**, *33* (5), 748-759.

- (3) Rice, O. K. Perturbations in Molecules and the Theory of Predissociation and Diffuse Spectra. II. *Physical Review* **1930**, *35* (12), 1551-1558.
- (4) Rice, O. K. Predissociation and the Crossing of Molecular Potential Energy Curves. *J. Chem. Phys.* **1933**, *I* (6), 375-389.
 - (5) Harris, R. A. Predissociation. J. Chem. Phys. 1963, 39 (4), 978-987.
- (6) Bixon, M.; Jortner, J. Intramolecular radiationless transitions. *J. Chem. Phys.* **1968**, *48* (2), 715-726.
- (7) Lefebvre-Brion, H.; Field, R. W. Perturbations in the Spectra of Diatomic Molecules. Academic Press, Orlando, 1986; pp 331-382.
- (8) Morse, M. D. Predissociation Measurements of Bond Dissociation Energies. *Acc. Chem. Res.* **2019**, *52*, 119-126.
- (9) Merriles, D. M.; Nielson, C.; Tieu, E.; Morse, M. D. Chemical Bonding and Electronic Structure of the Early Transition Metal Borides: ScB, TiB, VB, YB, ZrB, NbB, LaB, HfB, TaB, and WB. *J. Phys. Chem. A* **2021**, *125* (20), 4420-4434.
- (10) Morse, M. D.; Hansen, G. P.; Langridge-Smith, P. R. R.; Zheng, L.-S.; Geusic, M. E.; Michalopoulos, D. L.; Smalley, R. E. Spectroscopic studies of the jet-cooled nickel dimer. *J. Chem. Phys.* **1984**, *80*, 5400-5405.
- (11) Merriles, D. M.; Tomchak, K. H.; Ewigleben, J. C.; Morse, M. D. Predissociation measurements of the bond dissociation energies of EuO, TmO, and YbO. *J. Chem. Phys.* **2021**, *155* (14), 144303.
- (12) Spain, E. M.; Morse, M. D. Bond strengths of transition metal dimers: TiV, V₂, TiCo, and VNi. *J. Phys. Chem.* **1992**, *96*, 2479-2486.
- (13) Taylor, S.; Spain, E. M.; Morse, M. D. Spectroscopy and electronic structure of jet-cooled NiPd and PdPt. *J. Chem. Phys.* **1990**, *92*, 2710-2720.

- (14) Arrington, C. A.; Blume, T.; Morse, M. D.; Doverstål, M.; Sassenberg, U. Bond strengths of transition metal diatomics: Zr₂, YCo, YNi, ZrCo, ZrNi, NbCo, and NbNi. *J. Phys. Chem.* **1994**, *98*, 1398-1406.
- (15) Kramida, A.; Ralchenko, Yu.; Reader, J.; and NIST ASD Team, *NIST Atomic Spectra Database (version 5.10)*. National Institute of Standards and Technology, Gaithersburg, MD. https://dx.doi.org/10.18434/T4W30F, Accessed January, 2023.
- (16) Herzberg, G. Molecular Spectra and Molecular Structure I. Spectra of Diatomic Molecules. Van Nostrand Reinhold, New York, 1950.
- (17) Merriles, D. M.; Knapp, A. S.; Barrera-Casas, Y.; Sevy, A.; Sorensen, J. J.; Morse, M. D. Bond dissociation energies of diatomic transition metal nitrides. *J. Chem. Phys.* **2023**, *158* (8), 084308.
- (18) Johnson, E. L.; Davis, Q. C.; Morse, M. D. Predissociation measurements of bond dissociation energies: VC, VN, and VS. *J. Chem. Phys.* **2016**, *144* (23), 234306.
- (19) Brugh, D. J.; Morse, M. D.; Kalemos, A.; Mavridis, A. Electronic spectroscopy and electronic structure of diatomic CrC. *J. Chem. Phys.* **2010**, *133* (3), 034303.
- (20) Merriles, D. M.; Sevy, A.; Nielson, C.; Morse, M. D. The bond dissociation energy of VO measured by resonant three-photon ionization spectroscopy. *J. Chem. Phys.* **2020**, *153*, 024303.
- (21) Sorensen, J. J.; Tieu, E.; Sevy, A.; Merriles, D. M.; Nielson, C.; Ewigleben, J. C.; Morse, M. D. Bond dissociation energies of transition metal oxides: CrO, MoO, RuO, and RhO. *J. Chem. Phys.* **2020**, *153*, 074303.
- (22) Koukounas, C.; Kardahakis, S.; Mavridis, A. Ab initio investigation of the ground and low-lying states of the diatomic fluorides TiF, VF, CrF, and MnF. *J. Chem. Phys.* **2004**, *120* (24), 11500-11521.

- (23) Sevy, A.; Sorensen, J. J.; Persinger, T. D.; Franchina, J. A.; Johnson, E. L.; Morse, M. D. Bond dissociation energies of diatomic transition metal silicides: TiSi, ZrSi, HfSi, VSi, NbSi, and TaSi. *J. Chem. Phys.* **2017**, *147* (8), 084301.
- (24) Wu, Z. J.; Su, Z. M. Electronic structures and chemical bonding in transition metal monosilicides MSi (M=3d, 4d, 5d elements). *J. Chem. Phys.* **2006**, *124* (18), 184306.
- (25) Tong, G. S. M.; Jeung, G. H.; Cheung, A. S. C. Theoretical studies of the first-row transition metal phosphides. *J. Chem. Phys.* **2003**, *118* (20), 9224-9232.
- (26) Wu, Z. J.; Wang, M. Y.; Su, Z. M. Electronic structures and chemical bonding in diatomic ScX to ZnX (X = S, Se, Te). *J. Comput. Chem.* **2007**, *28* (3), 703-714.
- (27) Kardahakis, S.; Mavridis, A. First-Principles Investigation of the Early 3d Transition Metal Diatomic Chlorides and Their Ions, ScCl^{0,±}, TiCl^{0,±}, VCl^{0,±}, and CrCl^{0,±}. *J. Phys. Chem. A* **2009**, *113* (24), 6818-6840.
- (28) Balfour, W. J.; Qian, C. X. W.; Zhou, C. First observation and electronic spectroscopy of chromium mononitride: The A ⁴P_r X ⁴S⁻ transition near 745 nm. *J. Chem. Phys.* **1997**, *106* (11), 4383-4388.
- (29) Zhou, C.; Balfour, W. J.; Qian, C. X. W. The interacting B ⁴S⁻ and d²P states of CrN: A laser induced and dispersed fluorescence study. *J. Chem. Phys.* **1997**, *107* (12), 4473-4482.
- (30) Luo, Y.-R. Comprehensive Handbook of Chemical Bond Energies. CRC Press, Taylor and Francis Group, Boca Raton FL, 2007.
- (31) Panas, I.; Schule, J.; Brandemark, U.; Siegbahn, P. E. M.; Wahlgren, U. Comparison of the binding of carbon, nitrogen, and oxygen atoms to single nickel atoms and to nickel surfaces. *J. Phys. Chem.* **1988**, *92* (11), 3079-3086.
- (32) Daoudi, A.; Touimi Benjelloun, A.; Flament, J. P.; Berthier, G. Potential Energy Curves and Electronic Structure of Copper Nitrides CuN and CuN+Versus CuO and CuO+. *J. Mol. Spectrosc.* **1999**, *194* (1), 8-16.

- (33) Gutsev, G. L.; Andrews, L.; Bauschlicher, C. W., Jr. Similarities and differences in the structure of 3d-metal monocarbides and monoxides. *Theor. Chem. Acc.* **2003**, *109* (6), 298-308.
- (34) Merriles, D. M.; Tieu, E.; Morse, M. D. Bond dissociation energies of FeB, CoB, NiB, RuB, RhB, OsB, IrB, and PtB. *J. Chem. Phys.* **2019**, *151*, 044302.
- (35) Tzeli, D.; Mavridis, A. Electronic structure and bonding of the 3d transition metal borides, MB, M = Sc, Ti, V, Cr, Mn, Fe, Co, Ni, and Cu through all electron *ab initio* calculations. *J. Chem. Phys.* **2008**, *128* (3), 034309.
- (36) Ferrão, L. F. A.; Spada, R. F. K.; Roberto-Neto, O.; Machado, F. B. C. A multireference configuration interaction study of CuB and CuAl molecular constants and photoionization spectra. *J. Chem. Phys.* **2013**, *139* (12), 124316.
- (37) Merriles, D. M.; Tomchak, K. H.; Nielson, C.; Morse, M. D. Early Transition Metals Strengthen the B₂ Bond in MB₂ Complexes. *J. Am. Chem. Soc.* **2022**, *144* (17), 7557-7561.
- (38) Cheung, L. F.; Kocheril, G. S.; Czekner, J.; Wang, L.-S. The nature of the chemical bonding in 5d transition-metal diatomic borides MB (M = Ir, Pt, Au). *J. Chem. Phys.* **2020**, *152* (17), 174301.
- (39) Ouyang, Y.; Wang, J.; Liu, F.; Liu, Y.; Du, Y.; He, Y.; Feng, Y. Density functional study of 3d-transition metal aluminides. *J. Mol. Struct. THEOCHEM* **2009**, *905* (1-3), 106-112.
- (40) Yao, C.; Guan, W.; Song, P.; Su, Z. M.; Feng, J. D.; Yan, L. K.; Wu, Z. J. Electronic Structures of 5d Transition Metal Monoxides by Density Functional Theory. *Theor. Chem. Acc.* **2007**, *117* (1), 115-122.
- (41) Sorensen, J. J.; Tieu, E.; Morse, M. D. Bond dissociation energies of the diatomic late transition metal sulfides: RuS, OsS, CoS, RhS, IrS, and PtS. *J. Chem. Phys.* **2020**, *152*, 244305.
- (42) Sevy, A.; Tieu, E.; Morse, M. D. Bond dissociation energies of FeSi, RuSi, OsSi, CoSi, RhSi, IrSi, NiSi, and PtSi. *J. Chem. Phys.* **2018**, *149*, 174307.

- (43) Gingerich, K. A. Gaseous metal borides. III. Dissociation energy and heat of formation of gold monoboride. *J. Chem. Phys.* **1971**, *54* (6), 2646-2650.
- (44) Birge, R. T.; Sponer, H. The Heat of Dissociation of Non-Polar Molecules. *Physical Review* **1926**, *28* (2), 259-283.
- (45) Gaydon, A. G. The determination of dissociation energies by the Birge-Sponer extrapolation. *Proceedings of the Physical Society* **1946**, *58* (5), 525.
- (46) Schultz, R. H.; Elkind, J. L.; Armentrout, P. B. Electronic effects in C-H and C-C bond activation. State-specific reactions of Fe⁺ (⁶D,⁴F) with methane, ethane, and propane. *J. Am. Chem. Soc.* **1988**, *110* (2), 411-423.
- (47) Behm, J. M.; Brugh, D. J.; Morse, M. D. Spectroscopic analysis of the open 3d subshell transition metal aluminides: AlV, AlCr, and AlCo. *J. Chem. Phys.* **1994**, *101*, 6487-6499.
- (48) Behm, J. M.; Arrington, C. A.; Morse, M. D. Spectroscopic studies of jet-cooled AlNi. *J. Chem. Phys.* **1993**, *99*, 6409-6415.
- (49) Guo, L. First-Principles Study of Molecular Hydrogen Adsorption and Dissociation on Al_nCr (n = 1–13) Clusters. *J. Phys. Chem. A* **2013**, *117* (16), 3458-3466.
- (50) Behm, J. M.; Arrington, C. A.; Langenberg, J. D.; Morse, M. D. Spectroscopic analysis of jet-cooled AlCu. *J. Chem. Phys.* **1993**, *99*, 6394-6408.
- (51) Tzeli, D.; Karapetsas, I.; Merriles, D. M.; Ewigleben, J. C.; Morse, M. D. Molybdenum–Sulfur Bond: Electronic Structure of Low-Lying States of MoS. *J. Phys. Chem. A* **2022**, *126* (7), 1168-1181.
- (52) Sorensen, J. J.; Tieu, E.; Morse, M. D. Bond dissociation energies of lanthanide sulfides and selenides. *J. Chem. Phys.* **2021**, *154*, 124307.

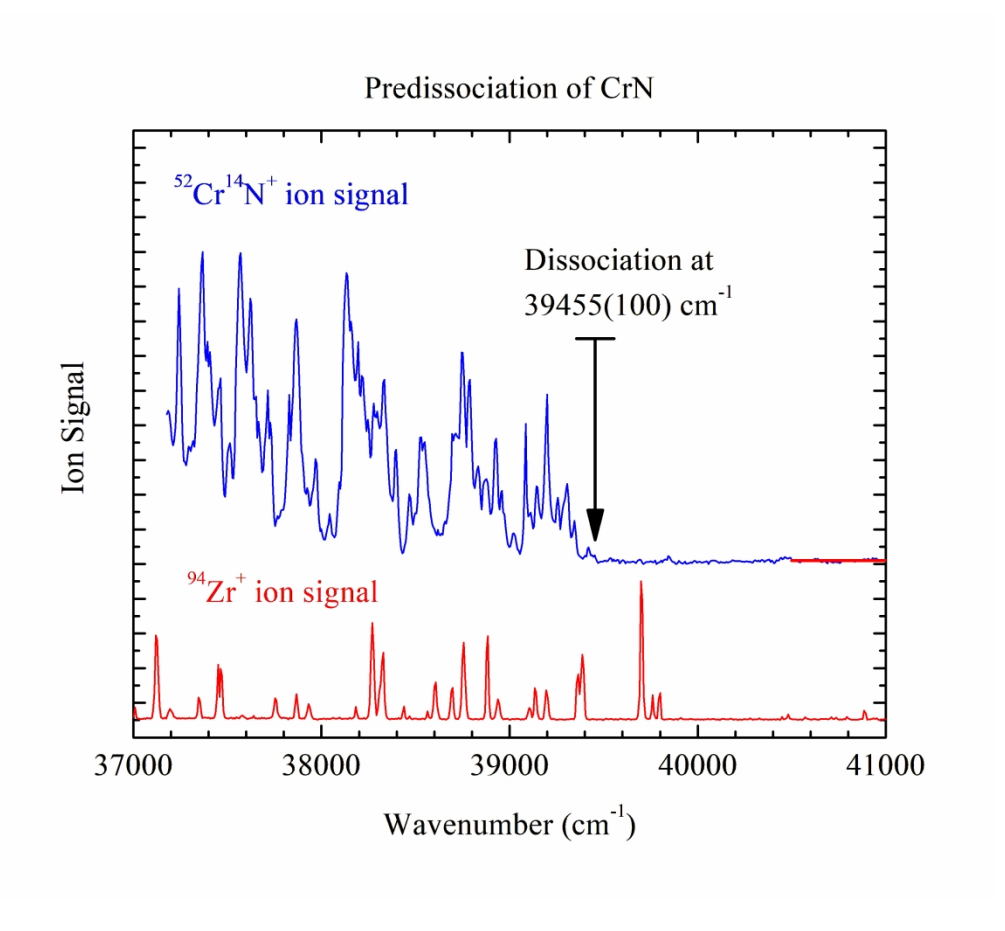


Figure 1. R2PI spectrum of CrN and its dissociation to an excited SAL. The upper, blue trace displays the measured $^{52}\text{Cr}^{14}\text{N}$ ion signal and its predissociation threshold at 39 455(100) cm $^{-1}$. The lower, red trace displays the ^{94}Zr atomic signal that was used to calibrate the spectrum.

245x217mm (300 x 300 DPI)

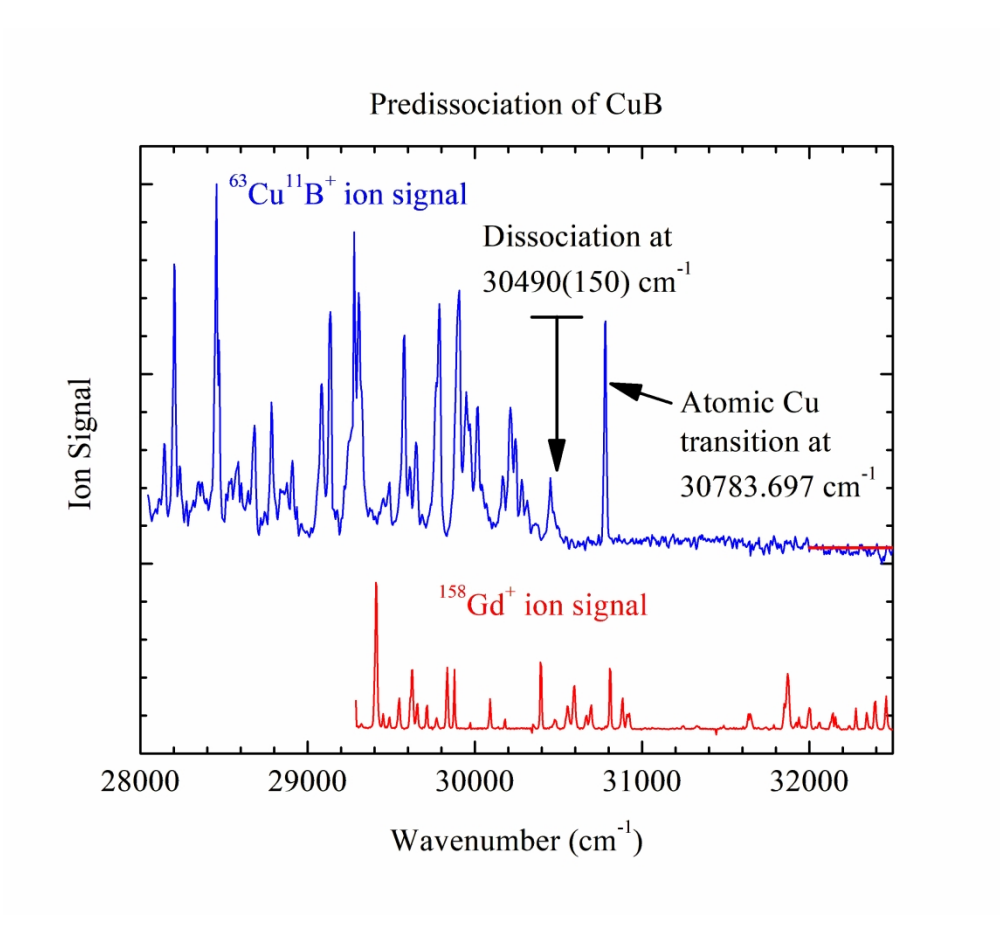


Figure 2. R2PI spectrum of CuB in the vicinity of its predissociation to an excited SAL. The top, blue trace displays the 63 Cu 11 B signal and its measured predissociation threshold at 30,490(150) cm $^{-1}$ or 3.780(19) eV. Also observed is a strongly allowed Cu atomic transition at 30 783.697 cm $^{-1}$ that caused an artificial increase in signal for CuB. 15 This is an unavoidable artifact of the R2PI technique. 37 The bottom, red trace shows the 158 Gd atomic transitions that were used to calibrate the wavenumber axis.

245x217mm (300 x 300 DPI)

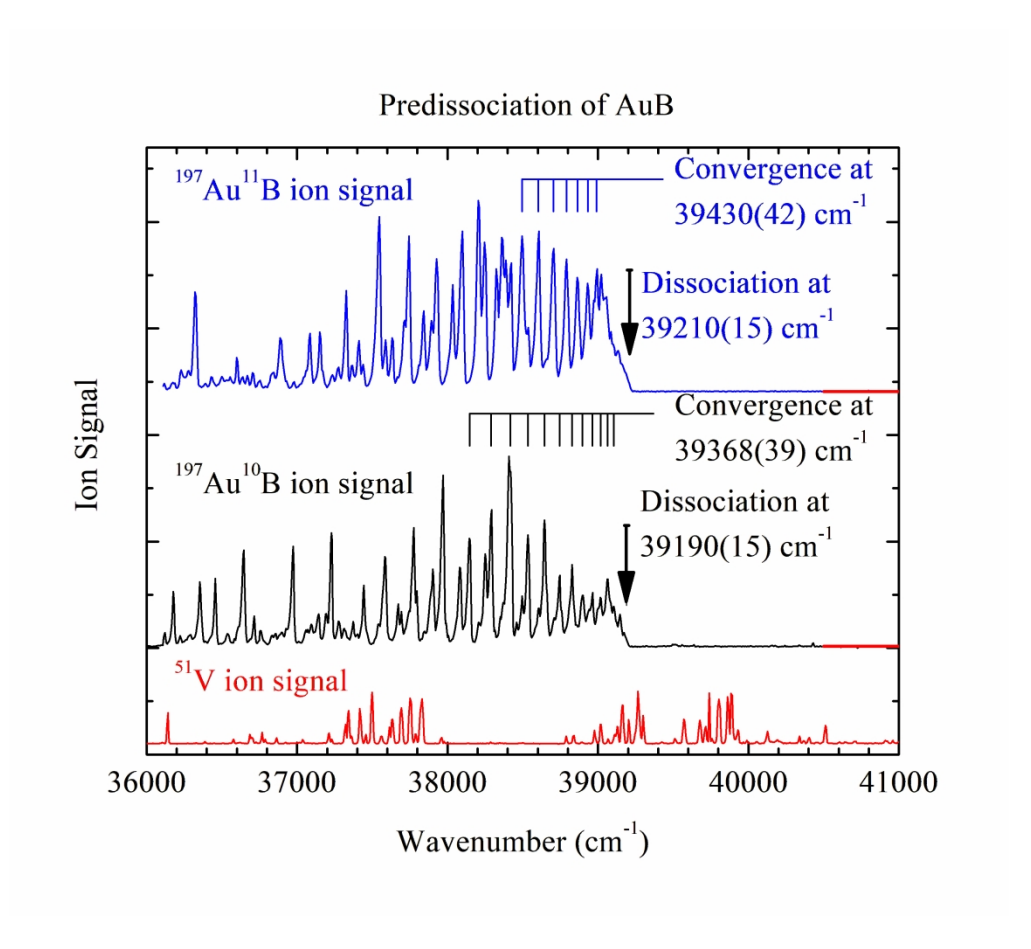


Figure 3. R2PI Spectrum of AuB in the energetic vicinity of its dissociation to the first excited limit of Au $5d^96s^2$, $^2D_{5/2g} + B \ 2p^1$, $^2P_{1/2}$, $_{3/2u}$. The top, blue trace displays the $^{197}Au^{11}B^+$ ion signal and its predissociation threshold at 39 210(15) cm $^{-1}$ or 4.861(2) eV. The middle, black trace shows the $^{197}Au^{10}B^+$ ion signal and its predissociation threshold at 39 190(15) cm $^{-1}$ or 4.859(2) eV. Vibrational progressions are identified above each spectrum and their convergence limits are listed. The bottom, red trace shows the ^{51}V atomic spectrum that was collected for calibration.

245x217mm (300 x 300 DPI)

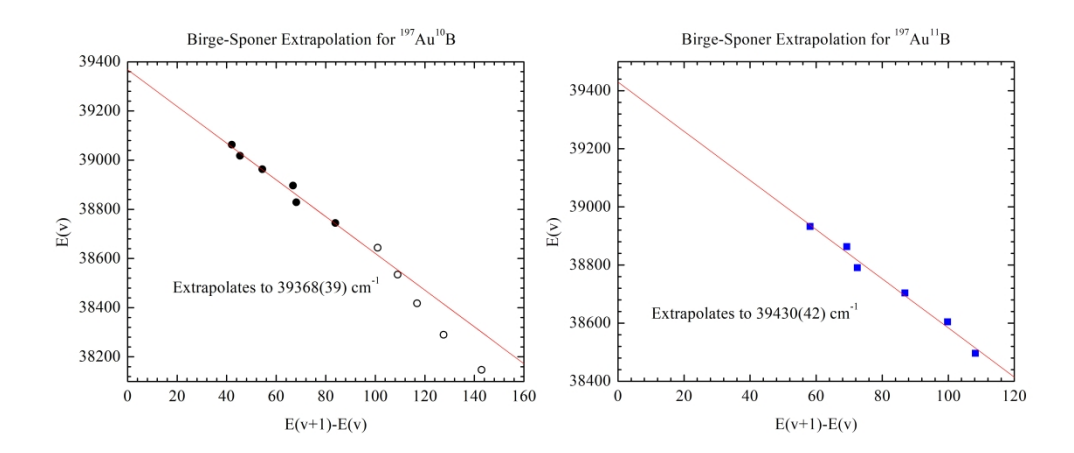
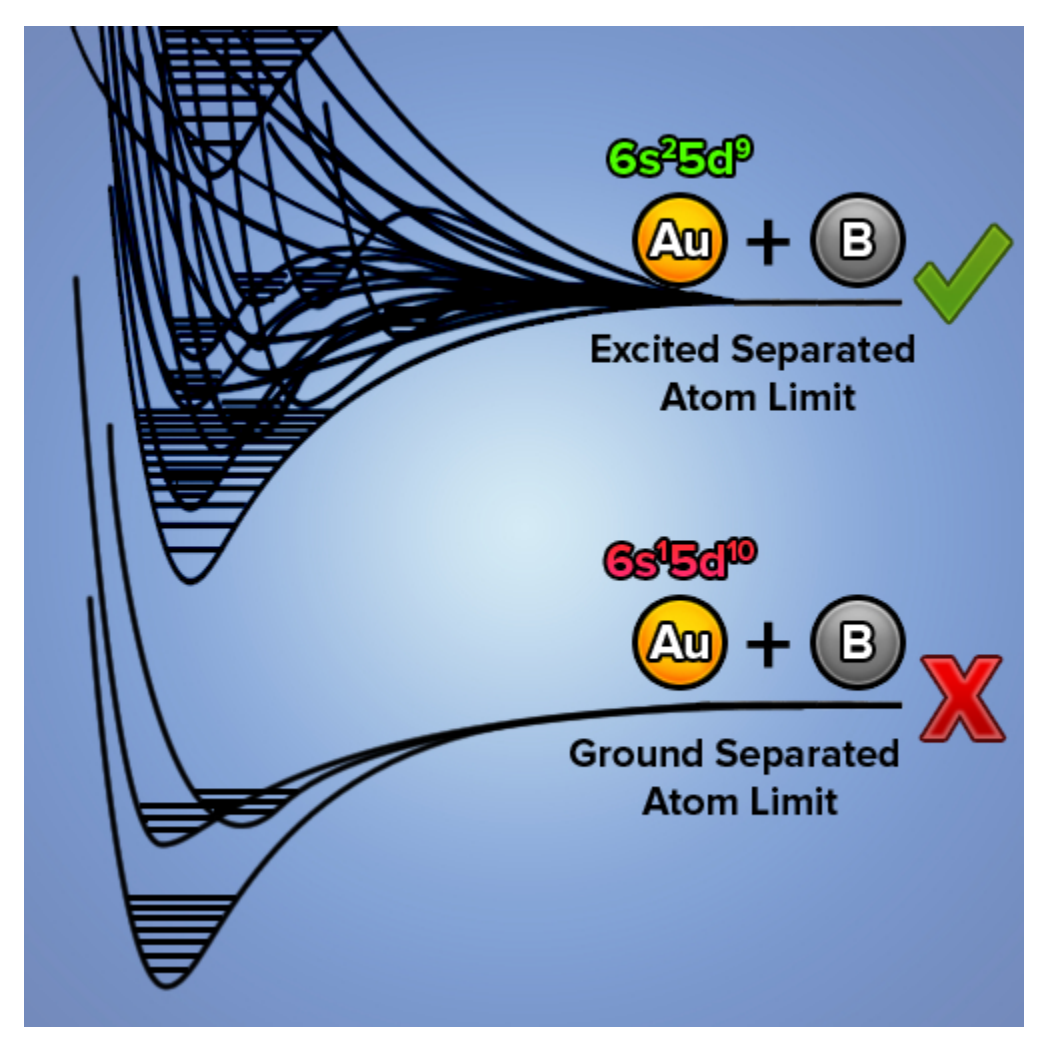


Figure 4. Left: The Birge-Sponer extrapolation performed for ¹⁹⁷Au¹⁰B, converging at 39 368(39) cm⁻¹. A total of 11 vibrational features were identified as part of the vibrational progression, represented by the 11 black circles. The six filled black circles were used in the linear fit, as the five unfilled black circles display a notably different slope. Right: The Birge-Sponer extrapolation performed for ¹⁹⁷Au¹¹B, converging at 39 368(39) cm⁻¹. The six blue squares represent the six vibrational features identified in the ¹⁹⁷Au¹¹B R2PI spectrum.

1942x848mm (72 x 72 DPI)



ToC figure 50x50mm (250 x 250 DPI)